Transactions, **SMiRT-26**
Berlin/Potsdam, Germany, July 10-15, 2022
Division IV

METHODS FOR SIMULATION OF HARD PROJECTILE IMPACT ON REINFORCED CONCRETE STRUCTURES

Lars Heibges[1], Pascal Distler[2], Hamid Sadegh-Azar[3]

[1] Research Assistant, Institute of Structural Analysis and Dynamics, University of Kaiserslautern, Kaiserslautern, Germany (lars.heibges@bauing.uni-kl.de)
[2] Research Assistant, Institute of Structural Analysis and Dynamics, University of Kaiserslautern, Kaiserslautern, Germany (pascal.distler@bauing.uni-kl.de)
[3] Professor, Institute of Structural Analysis and Dynamics, University of Kaiserslautern, Kaiserslautern, Germany (hamid.sadegh-azar@bauing.uni-kl.de)

ABSTRACT

Reinforced concrete (RC) protective walls, in particular those of nuclear or industrial installations, must be protected against unintentional or intentional impact scenarios such as aircraft crashes. In the worst-case scenario of an aircraft crash, local and global damage is caused to the structure. For a better understanding of the damage mechanisms, experimental tests as well as analytical and numerical models can be investigated. Based thereon the damage can be quantified and design guidelines developed.

The load-bearing capacity of RC slabs can be estimated by various methods and models. On the one hand, there are empirical and semi-empirical models which allow a fast calculation with few input parameters. On the other hand, validated Finite Element (FE) simulation models allow further investigation of damage mechanisms as well as detailed evaluation of stresses and strains in concrete and reinforcement.

This paper investigates the efficiency of existing analytical and empirical approaches as well as numerical simulation methods in predicting the load-bearing capacity of reinforced concrete structures under hard impact loads. Moreover, a novel simplified mechanical analytical method is proposed. The mechanical principles are based on a nonlinear two degree of freedom (TDOF) system by Schlüter (1987), which was extended for applications on hard impact scenarios. FE-simulations and experimental test results of recent and ongoing research projects are presented and have been used for validation purposes.

INTRODUCTION

The impacting missiles or projectiles can be classified as hard, semi-hard or soft, depending on the deformability of the missile relative to the target deformability. If the projectile is deformable relative to the target (soft missile) the assumptions of a plastic shock are a suitable approach and a load-time function can be determined using simplified methods, e. g. by Riera (1968). In the event of a hard impact, the contact actions and target reactions are strongly coupled and hence the calculation of capacity and damage effects is very sophisticated.

Therefore, if hard and non-deformable parts of a plane or engine (e. g. engine shaft) are investigated, the interaction between the RC structure and the impacting projectile should be considered. The rigid parts can be considered separately in these approaches e. g. by means of empirical formulas.

EMPIRICAL FORMULAS

Empirical formulas enable rapid estimation of damage parameters such as the perforation thickness or penetration depth. There are several formulas proposed by different institutes. Important input parameters are the mass of the projectile M_P, the impact velocity v_p, the projectile diameter D and the compressive strength f_c as well as the density of the concrete ρ_c. Only few formulas consider the reinforcement content r of the target slab.

Using the empirical formulas below (see equations (1) – (8)), the perforation thickness, i. e. the thickness of the target structure at which the projectile just perforates the RC slab, is determined.

Table 1: Empirical formulas

CEA-EDF (1974)	$t_p = 0{,}82 \cdot \frac{M_P^{\frac{1}{2}} \cdot v_p^{\frac{3}{4}} \cdot D}{\rho_c^{\frac{1}{8}} \cdot f_c^{\frac{3}{8}} \cdot D^{\frac{3}{2}}}$	(1)
CEA-EDF (Fullard)	$t_p = \left(\frac{v_p^{\frac{1}{2}}}{1{,}3 \cdot \rho_c^{\frac{1}{6}} \cdot f_c^{\frac{1}{2}} \cdot \left(\frac{D}{M_P}\right)^{\frac{2}{3}} \cdot (r+0{,}3)^{\frac{1}{2}}} \right)^{\frac{3}{4}}$	(2)
CEA-EDF (Li et al.)	$t_p = \left(\frac{v_p^{\frac{1}{2}}}{1{,}3 \cdot \rho_c^{\frac{1}{6}} \cdot f_c^{\frac{1}{2}} \cdot \left(\frac{D}{M_P}\right)^{\frac{2}{3}} \cdot (r+0{,}3)^{\frac{1}{2}} \cdot \left[1{,}2 - 0{,}6 \cdot \left(\frac{c_r}{t_d}\right)\right]} \right)^{\frac{3}{4}}$	(3)
Chang	$t_p = \left(\frac{61}{v_p}\right)^{\frac{1}{4}} \cdot \left(\frac{M_P \cdot v_p^2}{D \cdot f_c}\right)^{\frac{1}{2}}$	(4)
CRIEPI	$t_p = 0{,}9 \cdot \left(\frac{61}{v_p}\right)^{\frac{1}{4}} \cdot \left(\frac{M_P \cdot v_p^2}{D \cdot f_c}\right)^{\frac{1}{2}}$	(5)
NDRC/ Degen	$t_p = \alpha_p \cdot D \cdot \left(2{,}2 \cdot \frac{x_c}{\alpha_c \cdot D} - 0{,}3 \cdot \left(\frac{x_c}{\alpha_c \cdot D}\right)^2\right)$	(6)
AFCEN-RCC	$t_p = \left(\frac{M_P}{\rho_c \cdot D} \cdot \left(\frac{1}{1{,}89} \cdot \left(\frac{\rho \cdot v_p^2}{10^6 \cdot f_c}\right)\right)^{\frac{3}{4}}\right)^{\frac{1}{2}}$	(7)
AFCEN-RCC extended	$t_p = \left(\frac{v_p^2}{1{,}9 \cdot f_c \cdot \rho_c^{\frac{1}{3}} \cdot \left(0{,}35 \cdot \left(\frac{r}{200}\right)^{\gamma} + 0{,}65\right)^2 \cdot \left(\frac{f_c}{36 \cdot 10^6}\right)^{-\frac{1}{2}}} \right)^{\frac{3}{8}} \cdot \sqrt{\frac{M_P}{D}}$	(8)

LIMITS OF APPLICATION

A major part of the formulas is based on experimental investigations. Therefore, the application range must be observed. Table 2 gives an overview of the application limits of the presented formulas.

Table 2: Limits of application of the formulas

CEA-EDF (1974)	$v < 200\ m/s$ $23\ MPa < f_c < 46\ MPa$ $20\ kg < M_P < 300\ kg$ $D \leq 0{,}3\ m$ $0{,}35 < D/t_d < 4{,}17$	**CEA-EDF (Fullard)**	$45\ m/s < v < 300\ m/s$ $15\ MPa < f_c < 37\ MPa5$ $0{,}33 < D/t_d < 5$ $0 < r < 0{,}75\ \%\ each\ way\ each\ face$
Chang	$16\ m/s < v < 311{,}8\ m/s$ $22{,}8\ MPa < f_c < 45{,}5\ MPa$ $0{,}0508\ m < D < 0{,}3048\ m$ $0{,}11\ kg < M_P < 342{,}9\ kg$	**CEA-EDF (Li et al.)**	$11\ m/s < v < 300\ m/s$ $f_c < 37\ MPa$ $0{,}33 < D/t_d < 5$ $0 < r < 0{,}75\ \%\ each\ way\ each\ face$ $0{,}12 < c_r/t_d < 0{,}49$ $150\ kg/m^3 < M_P/(U/2)^2 \cdot t_d < 10^4\ kg/m^3$
CRIEPI	$16\ m/s < v < 311{,}8\ m/s$ $22{,}8\ MPa < f_c < 45{,}5\ MPa$ $0{,}0508\ m < D < 0{,}3048\ m$ $0{,}11\ kg < M_P < 342{,}9\ kg$	**AFCEN-RCC**	$v > 20\ m/s$ $25\ MPa < f_c < 45\ MPa$ $0{,}5 < D/t_d < 3{,}3$ $0{,}5 < M_P/(\rho \cdot {t_d}^2) < 5$ $100\ kg/m^3 < reinforcement$ $< 250\ kg/m^3$
NDRC/ Degen	$25\ m/s < v < 311{,}8\ m/s$ $28{,}4\ MPa < f_c < 43{,}1\ MPa$ $0{,}1\ m < D < 0{,}31\ m$ $0{,}15\ m < t_d < 0{,}61\ m$	**AFCEN-RCC extended**	$v < 250\ m/s$ $15\ MPa < f_c < 80\ MPa$ $0{,}25 < D/t_d < 3{,}3$ $symmetrical\ reinforcement$

SIMULATION OF SOFT MISSILE IMPACT

The CEB-model (Comité Euro-International du Béton) according to Schlüter (1987) and CEB (1988) is considered a useful and simplified solution for estimating the load-bearing capacity of reinforced concrete plates subjected to soft missile impact. This analytical model describes all relevant mechanisms in a physically adequate manner and allows a fast evaluation of the system response under missile impact. The reinforced concrete plate is represented as a two-degree of freedom (TDOF) system with the following equations of motion (see equations (9) and (10), figure 1).

$$M_1 \cdot \ddot{w}_1 + c_1 \cdot \dot{w}_1 + R_1(w_1) - R_2(u) - c_2 \cdot \dot{u} = 0 \tag{9}$$

$$M_2 \cdot \ddot{w}_2 + c_2 \cdot \dot{u} + c_3 \cdot \dot{w}_2 + R_2(u) - F(t) = 0 \tag{10}$$

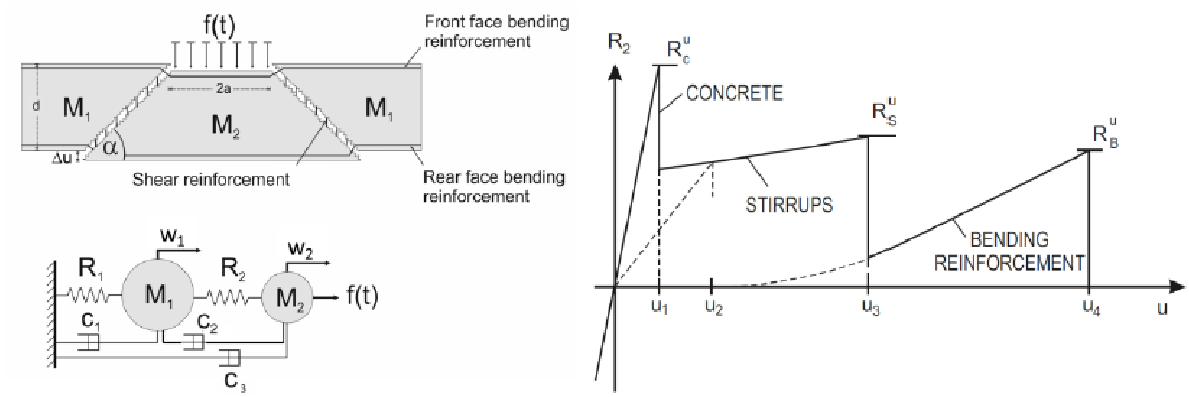

Figure 1. CEB model and the three components of local resistance R_2 (Distler 2021).

Nonlinear springs and dampers couple two masses. M_1 and $R_1(w_1)$ represent the deformation characteristics of a circular plate in bending while M_2 and $R_2(u)$ represent the local behaviour of the punching cone in the area of impact relative to the rest of the plate ($u = w_2 - w_1$). Damping is also included in this model to represent the amount of energy dissipation from internal damage of the concrete and the dowel action of the bending reinforcement. Initially, the assumed punching cone M_2 is monolithically connected to the remaining concrete slab. The resistance R_1 is idealized as an elastoplastic spring describing bending of the plate. When the concrete tensile strength is exceeded, depending on the reinforcement content, separation of punching cone and slab occurs. The resistance $R_2(u)$ consists of three components, which can be idealized as three parallel connected springs, describing the contribution of the concrete, the stirrups and the bending reinforcement. Figure 1 clarifies the three components of the local resistance $R_2(u)$.

SIMULATION OF HARD MISSILE IMPACT

If only non-deformable parts of a plane or engine are investigated, called hard missiles, the interaction between the target and the impacting projectile as well as the process of penetration of the projectile need to be considered (see figure 2). As the original CEB model according to Schlüter (1987) only works with soft missiles, the approaches should be modified.

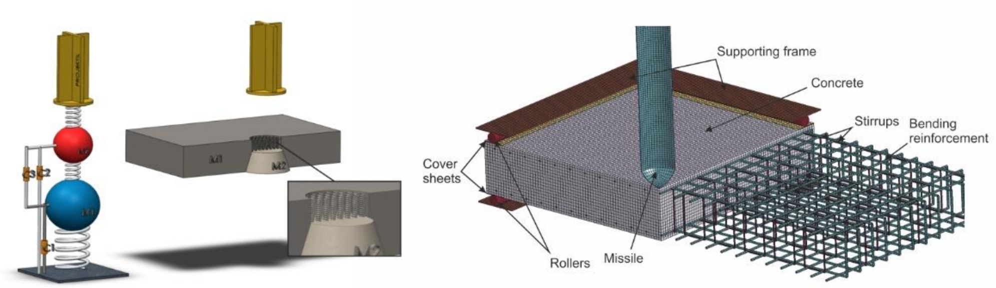

Figure 2. Model for missile impact (left); FE model of selected impact test (right) (Distler 2021).

Load Interaction

To determine the target response to a hard missile impact, it is desirable to know the impact force-time-history or at least the duration of impact. Using the approach of Jonas and Rüdiger (1974), the time-history of the impact force can be approximated by equation (12). This approach results from the integration of the equation of motion which is given in equation (11).

$$M_P \cdot a = -F_i = -c \cdot x \cdot v \tag{11}$$

$$F(t_i) = \frac{2 \cdot M_P \cdot v_P^2}{x_c} \cdot \tanh\left(\frac{v_P \cdot t_i}{x_c}\right) \cdot \left[1 - \tanh\left(\frac{v_P \cdot t_i}{x_c}\right)^2\right] \tag{12}$$

Where M_P is the mass of the projectile, v_p is the impact velocity and c is a factor to be determined experimentally. A prerequisite for a useful load-approach function according to Jonas and Rüdiger (1974) is an accurate determination of the penetration depth x_c of the projectile into the target structure using the empirical formulas presented in table 1 or experimental data. The formula is derived for SI units and must be converted consistently if necessary.

Regarding the load interaction of the projectile and the RC slab, the impact process should be considered in two different phases. At first, the projectile penetrates the RC structure and creates an almost cylindrical penetration form as long as the concrete spring R_c^u is active. Therefore, the penetration depth x_i due to the projectile decreases the total slab thickness d at each time step t_i (see figure 3). In order to consider this adjustment for hard missile impacts, the load-bearing capacity of the concrete R_c^u is modified from the original CEB model in equation (13).

$$R_c^u = \left[\left(a + \frac{d - x_i}{\tan(\alpha)}\right)^2 - a^2\right] \pi \cdot f_{ct} \tag{13}$$

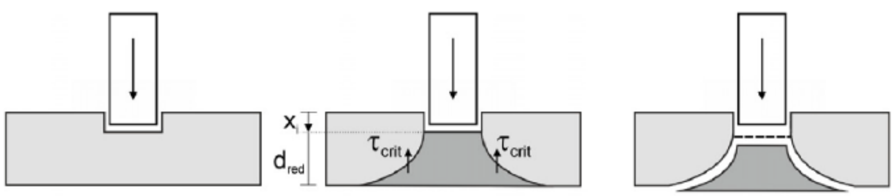

Figure 3. Phases of penetration process.

In equation (13) a is the projectile radius and f_{ct} represents the tensile strength of concrete. The effective height of the plate h_{eff} is also reduced resulting in a decrease in fracture deformation of u_1 (see equations (14) and (15)).

$$h_{eff} = 0{,}5 \cdot (d - x_i) \tag{14}$$

$$u_1 = h_{eff} \cdot \frac{2}{3} \cdot \frac{f_{ct}}{E_c} \tag{15}$$

Adjustment of the mass of the punching cone

In the CEB model, the mass of the punching cone M_2 is calculated on the assumption of a linear cone shape. Experimental investigations concerning the punching cone in Just et al. (2016) and NEA (2012) have shown a dependence between the shape of the punching cone and the function of projectile speed as well as plate thickness d. To improve the calculation of M_2, the shape of the cone will be estimated with an exponential shape function based on an input parameter β shown in equation (16) and visualized in figure 4.

$$s_f(d_i) = d \cdot \left(c \cdot e^{\left(\frac{1}{\beta}\right) \cdot \left(\frac{x_i}{d}\right)} - b\right) \tag{16}$$

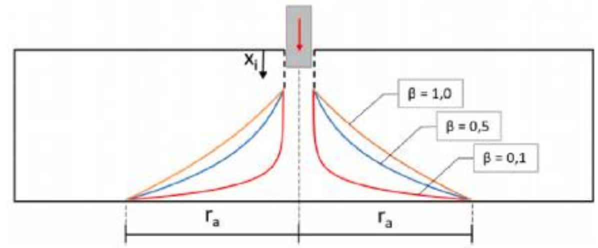

Figure 4. Shear fracture zone.

In equation (16), d is the slab thickness and r_a is the assumed punching cone radius. The parameter c and b are fixed values that are defined by the boundary values of the function, $s_f(x_i) = 0{,}5 \cdot D$ and $s_f(d) = r_a$.

The application of the exponential shear fracture zone is illustrated with the VTT tests A1 and IRIS P1 for determining the mass M_2 according to equation (16) in figure 5.

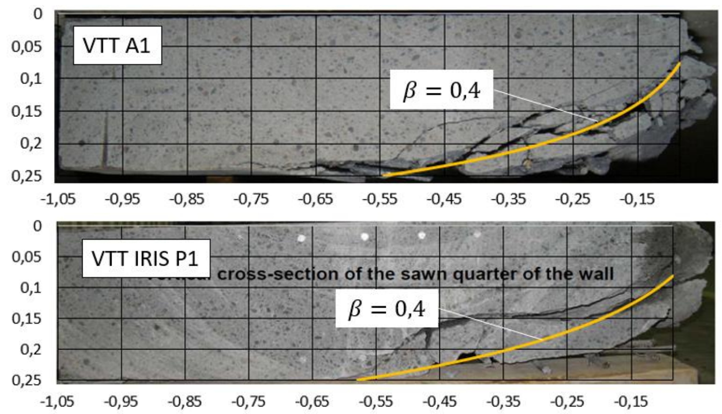

Figure 5. Cross-section of the RC structure as well as the assumed punching cone shape.

Adjustment of the effective mass

The calculation of the effective mass M_{eff} of the RC slab has significant influence on the global response of the system. Depending on the boundary conditions of the target structure a mass factor μ must be adjusted (see equation 17)).

$$M_{eff} = \mu \cdot M_{total} \tag{17}$$

If there is experimental data concerning the displacements of the RC plate in longitudinal or transversal direction, a shape function $\varphi(x, y)$ of the deformation of the slab can be approximated (see figure 6). Integration of the shape function in both x and y directions yields the equivalent mass M_{eq} according to equation (18). The ratio of equivalent mass M_{eq} and total mass M_{total} is described as mass factor μ (see equation (19)).

$$M_{eq} = \rho_{concrete} \cdot d \iint_0^L \left(\phi(x, y)\right)^2 \, dy \, dx \tag{18}$$

$$\mu = \frac{M_{eq}}{M_{total}} \tag{19}$$

A simplified approach is presented by Biggs (1964). For different boundary conditions, mass factors are suggested depending on the damage level. Table 3 shows the experimental results and the suggestion by Biggs (1964) for simply supported two-way slabs.

Table 3. Mass factor μ according to Biggs (1964) and experimental data.

Test	μ (exp.)	μ (Biggs)	Restraints
VTT A1	0,23	0,17 (plastic) 0,31 (elastic)	Rectangular supported at all edges
VTT P1	0,26		
M284	0,30		
M171	0,30		

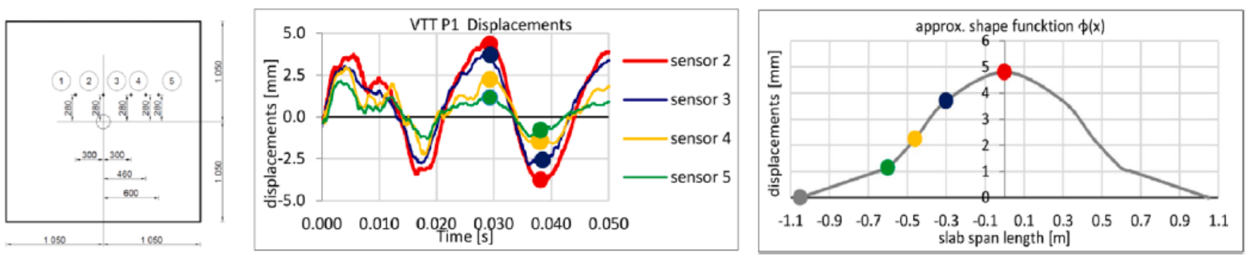

Figure 6. Evaluation of shape function (Distler 2021).

STUDIES ON SELECTED IMPACT TESTS

Table 4 shows the test data of the selected impact tests conducted by the Technical Research Centre VTT (see Heckötter and Sievers (2016) and Heckötter and Vepsä (2015)) of Finland.

Table 4. Test data of impact tests.

Test	M_P [kg]	v_p [m/s]	D [m]	Dimensions [m]	f_c [N/mm²]	Reinforcement [%]
VTT A1	47,5	101	0,1683	2,10 x 2,10 x 0,25	60	0,35
VTT P1	47,5	102,2	0,1683		40,6	0,35

For VTT A1 and VTT P1 the perforation thickness is determined in figure 7 using the presented empirical formulas. While the CEA and RCC formulas are in good agreement with the experimental data, the NDRC, CRIEPI and Chang formula slightly overestimate the load-bearing capacity of the RC slab for these tests.

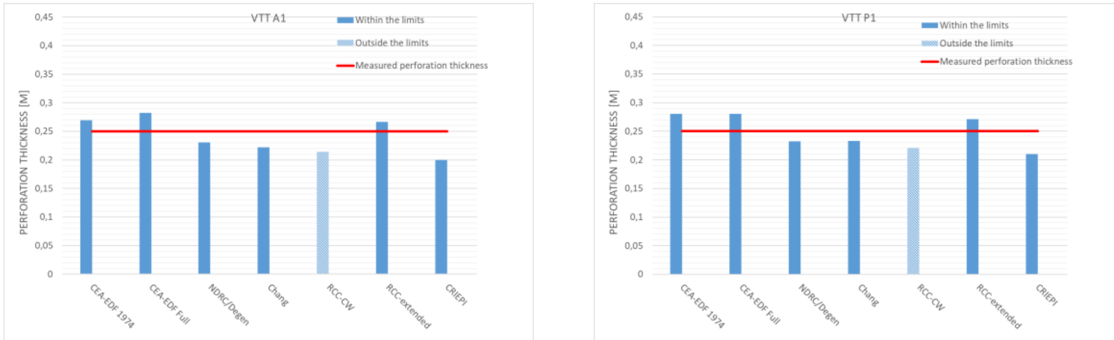

Figure 7. Evaluation of perforation thickness.

Experimental data as well as numerical results of the tests VTT A1 and VTT P1 are used for verification purposes of the simplified mechanical analytical model. First, based on the measured penetration depth, the load-time function for the selected impact tests VTT A1 and VTT P1 is calculated according to Jonas and Rüdiger (1974).

In test VTT P1, the hard missile perforates the RC slab. The calculation of the adjusted CEB model results in the damage mode 'perforation', as both the upper and lower bending reinforcement have reached their ultimate strain (see figure 8). The analytical calculation overestimates the damage to the RC slab. The frequency is in good agreement with the experimental as well as numerical data as figure 8 shows.

In test VTT A1, the ultimate load capacity of the target slab was not exceeded as the local spring R_2 seems to be intact in the analytical model (see figure 9). The displacement-time history visualized in figure 9 shows that the global damage is slightly overestimated. The overall target response of the adjusted CEB model is in good agreement with the experimental and numerical data.

The FE simulations shown in figures 8 and 9 reproduce the experimental damage mode. The frequency is too high.

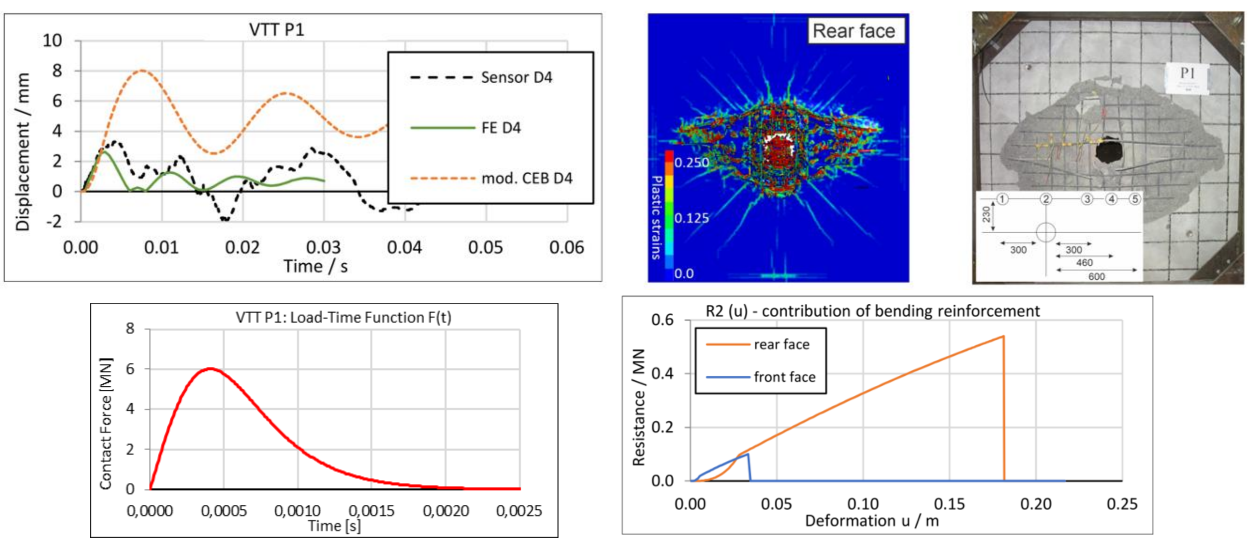

Figure 8. Calculated and measured deformation and load-time function of VTT P1.

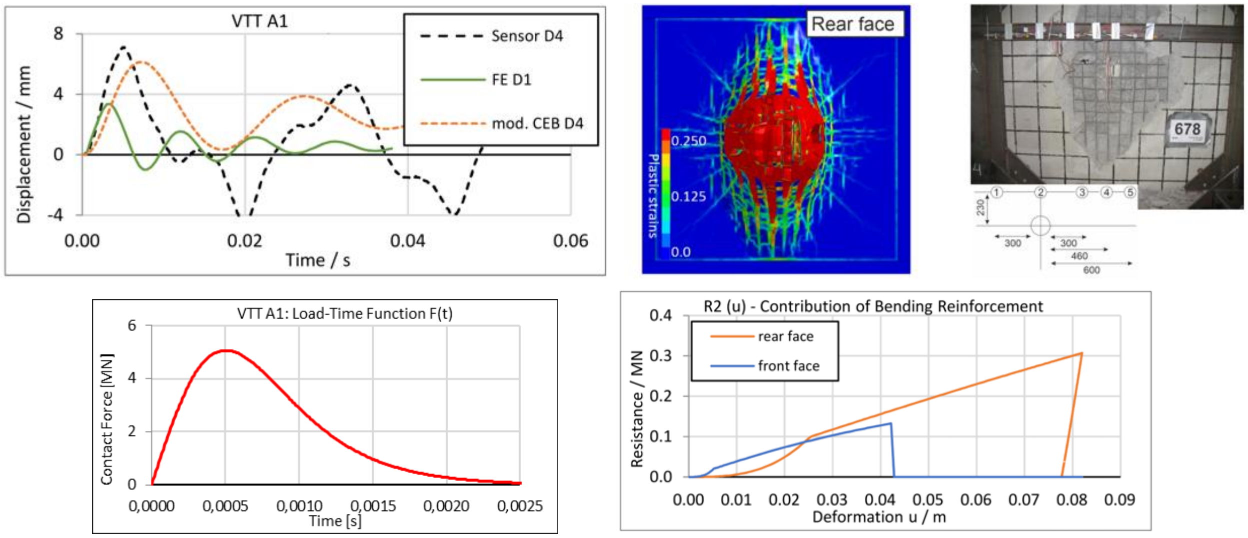

Figure 9. Calculated and measured deformation and load-time function of VTT A1.

CONCLUSION

In this paper, the efficiency of existing analytical and empirical as well as numerical simulation methods in predicting the load-bearing capacity of RC structures under impact loads is investigated. The presented empirical formulas allow a valid estimation of parameters such as the perforation thickness or the penetration depth. The considered VTT tests, especially the extended RCC as well as the CEA-EDF formulas enable a conservative estimation of the perforation thickness.

In addition, the paper presents adjustments for the CEB model for application on hard missile impact. Test data of the Technical Research Centre VTT in Finland and of the British Atomic Energy Agency UKAEA is used to determine the validity of the adjustments.

For verification purposes of the adjusted analytical model, the results of the experimental tests VTT A1 and VTT P1 as well as validated FE simulation models are used. The comparison between the analytical model, FE simulations and measured data shows good agreements. It was found that the adjusted CEB model for hard impacts can describe the essential behaviour of reinforced concrete slabs. An advantage of the analytical model is the fast applicability so that parameter studies can be carried out easily and quickly and that they complement complex procedures. It should be noted that particular input parameters such as the punching angle and damping are assumed. In addition to that, the load approach by Jonas and Rüdiger (1974) requires a sufficiently precise determination of the penetration depth. In order to increase the reliability of the analytically calculated results, the adjusted CEB model should be tested on a larger experimental base.

ACKNOWLEDGEMENT

The work has been performed within the framework of the Reactor Safety Research Program of the German Federal Ministry of Economic Affairs and Climate Action BMWK.

REFERENCES

Barriaud, C., Sokolovsky, A., Gueraud, R., Dulac, J., Labrot, R. (1978). “Local behaviour of reinforced concrete walls under missile impact”, Paper J 7/9, Fourth International Conference on Structural Mechanics in Reactor Technology, Berlin, Germany.

Biggs, J. M. (1964). “Introduction to Structural Dynamics”, Massachusetts Institute of Technology, USA.

Bracklow, F., Babiker, A., Hering, M., Kühn, T., Curbach, M. and Häußler-Combe, U. (2021). "Behaviour of structural components during impact load conditions caused by tank collisions (aircraft fuel tanks) – Phase 1C: Experimental and numerical study of scale effects and damage behaviour", Final Report Reactor safety research Project No. 1501541, University of Dresden, Germany.

Comité Euro-International du Béton (1988). "Concrete Structures under Impact and Impulsive Loading", *Bulletin d'Information no. 187*, Lausanne, Switzerland.

Distler, P., Sadegh-Azar, H., Heckötter, C. (2021). "Enhancement of engineering models for simulation of soft, and hard projectile impact on reinforced concrete structures", *Nuclear Engineering and Design*, Volume 378.

Fang, Q., Wu, H. (2017). "Concrete Structures Under Projectile Impact", Singapore, Singapore.

French Association for Design, Construction, and In Service Inspection Rules for Nuclear Island Components (afcen) (2016). "ETC-C EPR Technical code for civil works", 2012 Edition, Paris, France.

Heckötter, C., Sievers, J. (2015). "Weiterentwicklung der Analysemethodik zur Berücksichtigung komplexer Lastannahmen bei hochdynamischen Einwirkungen auf Stahlbetonstrukturen", Gesellschaft für Anlagen- und Reaktorsicherheit (GRS) gGmbH, Final Report, GRS-410, Cologne, Germany.

Heckötter, C., Vepsä, A. (2015). "Experimental investigation and numerical analyses of reinforced concrete structures subjected to external missile impact", *Progress in Nuclear Energy*, Amsterdam, Netherlands.

HOCHTIEF AG (1984). "Kinetische Grenztragfähigkeit von Stahlbetonplatten", BMFT Forschungsvorhaben RS 165, Schlussbericht.

HOCHTIEF AG (1984). "Kinetische Grenztragfähigkeit von Stahlbetonplatten", BMFT Forschungsvorhaben 1500408/ RS 467, Meppener Versuche Teil II.

Jonas, W., Rüdiger, E. (1974). "Dimensionierung von Stahlbetonbauteilen des äußeren Containments von Kernkraftwerken unter der Wirkung von Flugkörpern", BMFT Forschungsvorhaben RS 116

Just, M., Curbach, M., Kühn, T., Hering, M. (2016). "Bauteilverhalten unter stoßartiger Beanspruchung durch aufprallende Behälter (Flugzeugtanks)", Technical University of Dresden, Germany.

Nuclear Energy Institute (2011). "Methodology for Performing Aircraft Impact Assessments for New Plant Designs", Walnut Creek, California, USA.

Nuclear Energy Institute (2012). "Improving Robustness Assessment Methodologies for Structures Impacted by Missiles (IRIS_2010)", Final Report NEA/CSNI/R/(2011)8.

Riera, J. D. (1968). "On the Stress Analysis of Structures Subjected to Aircraft Impact Forces", *Nuclear Engineering and Design, Vol. 8*, Amsterdam, Netherlands.

Schlüter, F. H. (1987). "Dicke Stahlbetonplatten unter stoßartiger Belastung – Flugzeugabsturz", PhD thesis, University of Karlsruhe, Germany.